Biochemistry

 Volume 39, Number 21 May 30, 2000

Current Topics

Chemical Basis for Enzyme Catalysis

Thomas C. Bruice*,‡ and Stephen J. Benkovic*,§

Department of Chemistry and Biochemistry, University of California at Santa Barbara, Santa Barbara, California 93106, and Department of Chemistry, The Pennsylvania State University, University Park, Pennsylvania 16802

Received February 16, 2000; Revised Manuscript Received April 12, 2000

Some half-century ago Pauling (*1*, *2*) proposed that the lowering of the activation energy in enzyme catalysis stems from the enzyme's affinity for the transition state exceeding it's affinity for the substrate. This proposal has great popular appeal and has served as the basis for the design of transition state based inhibitors and for inducing catalytic activity in various molecular templates (*3*−*5*). Recent investigations, however, have brought into focus the contributions of thermal motions and ground state conformers associated with the Michaelis complex to the rate of enzymatic reactions (*6*, *7*). A description and analysis of the enzyme−substrate complex characteristics are a focus of this review.

The pseudothermodynamic cycle of Scheme 1 has been used to calculate the equilibrium constants ($1/K_{TS}$) for binding of various transition states by their respective enzymes. This simple cycle is subject to overinterpretation. The numerical value calculated for K_{TS} [$=(k_{non}K_m)/k_{cat}$] is one measure of the efficiency of catalysis and, therefore, is dependent on all factors in the enzymatic and nonenzymatic reactions. For instance, in the comparison of the difference of the free energy of interaction between E and S versus E and TS, one must take into account differences in the free energy of interaction of the solvent environment with S and TS in the presence and absence of E (*7*).

Wolfenden observed that the ratios of k_{cat}/k_{non}, for a series of enzymatic reactions, are determined primarily by k_{non} and that values of k_{cat} reside in a rather narrow range (Figure 1) (*3*). That the narrow range of log k_{cat} values does not correlate with the much larger range of log K_{TS} (slope 0.16) (*6*) is contrary to Pauling's proposal that the tighter the enzyme binds the transition state the greater the rate of catalysis. Unexpectedly, it is log k_{non} which shows a strong dependence

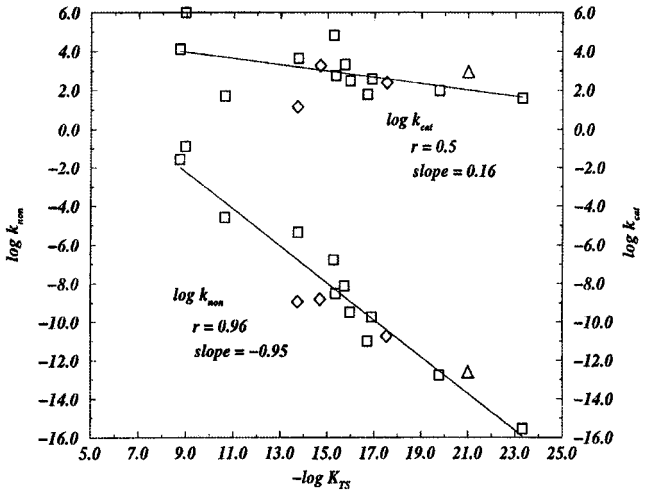

FIGURE 1: Comparison of the relationship of K_{TS} with the enzymatic reaction rate constant, k_{cat}, and with the uncatalyzed solution or reference reaction rate constant, k_{non}. Rate and equilibrium constants are defined in Scheme 1.

Scheme 1

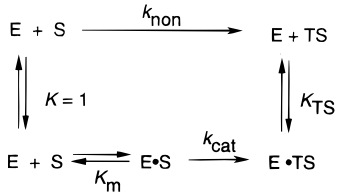

* Corresponding author. Telephone: (805) 893-2044. Fax: (805) 893-2229. E-mail: tcbruice@bioorganic.ucsb.edu.
‡ University of California at Santa Barbara.
§ The Pennsylvania State University.

10.1021/bi0003689 CCC: $19.00
Published on Web 05/05/2000

Table 1:[a] Enthalpies of Activation for Enzyme-Catalyzed (k_{cat}) and Nonenzymatic (k_{non}) Reactions

reaction	$\Delta H^{\ddagger}$ (k_{cat})	$\Delta H^{\ddagger}$ (k_{non})
yeast OMP decarboxylase	11	44.4
urease	9.9	32.4
bacterial α-glucosidase	10.5	29.7
staphylococcal nuclease	10.8	25.9
chymotrypsin	8.6	24.4
chorismate mutase	12.7	20.7

[a] See ref 8.

upon log K_{TS} (slope −0.95) (*6*). As k_{non} decreases the efficiency of catalysis (K_{TS}) increases such that values of k_{cat} span a defined range ($10-10^6$). This may be indicative of the need for metabolic processes to function within a defined time period so that k_{cat} must fall within this time period for an enzymatic reaction to be useful.

Preorganization and Activation Parameters in Intramolecular and Enzyme Catalysis. The increase in rate when a bimolecular reaction is converted to a first-order reaction by bringing the reactants together in a complex or a compound depends on the preorganization of the resulting complex or compound. The decrease in $\Delta G^{\ddagger}$ may be reflected in changes of both enthalpy and entropy terms. The narrow range of enzyme k_{cat} constants is reflected in a narrow range of associated values of $\Delta H^{\ddagger}$. This is shown in Table 1, which lists $\Delta H^{\ddagger}$ for both spontaneous (pH-independent) first-order reactions in water (k_{non}) and related single substrate enzyme reactions (k_{cat}) (*3*, *8*). Values of $T\Delta S^{\ddagger}$ average −4.6 and −4.0 kcal/mol at 25 °C for the enzymatic reactions and for the spontaneous reactions, respectively. The change in $\Delta H^{\ddagger}$ predominates over that for $T\Delta S^{\ddagger}$ in the determination of $\Delta G^{\ddagger}$ for these enzymatic reactions. This finding does not support the concept that enzymatic reactions are generally entropy driven (*9*). Entropic contributions might be expected to be more pronounced for multiple substrate−enzyme reactions (*10*). This remains to be examined experimentally. A compensation in the two terms has been anticipated (*11*).

Perhaps the most powerful insights into the question of the importance of transition state binding (*12*) vs ground state effects comes from modern computational methods. An understanding of the dependence of the efficiencies of both intramolecular and enzymatic reactions upon structural preorganization requires examination of the time-dependent dynamic motions and conformational structures of ground states compared to transition states.

The relationship between the observed rate constants and molecular structure for a series of intramolecular reactions which share a common transition state (TS), but differ in the preorganization of the ground state, has been investigated through computational methods (stochastic search with molecular mechanics for the ground state and semiempirical plus ab initio quantum mechanics for the transition state). These reactions involve intramolecular nucleophilic displacement of RO^- from −COOR by $-CO_2^-$ to provide cyclic anhydrides −C(=O)OC(=O)− (*7*, *13*, *14*). In order for the reaction to take place, ground state conformers which closely resemble the transition state (near attack conformers, NACs)[1] must be formed. NACs may be considered as turnstiles through which the ground state must pass to enter the transition state. The geometry of a NAC for this reaction is shown in Chart 1.

Chart 1

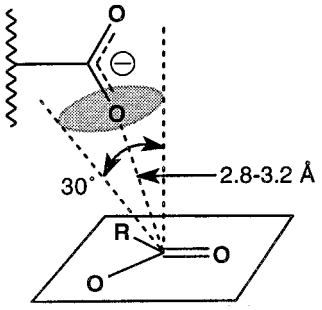

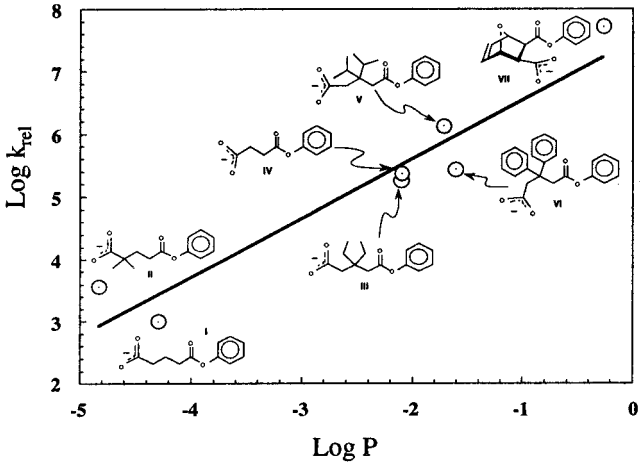

FIGURE 2: Log of the relative rate constants (k_{rel}) for anhydride formation from mono-*p*-bromophenyl esters vs the log of the probability (*P*) for NAC formation of each monophenyl ester of the various dicarboxylic acids.

By knowing the structures of all ground state conformations and their energies, the mole fraction (*P*) of conformers present as NACs was derived for each carboxylate monoester using the Boltzmann distribution equation (*13*). In Figure 2 the log of the rate constant for cyclization can be seen to be a linear function of log *P*. Thus, the $\Delta G^{\ddagger}$ of each intramolecular reaction is directly dependent on the fraction of ground state conformations present as NACs. The differences in *P* for the various reactions reflect the extent of preorganization of the structures. The better the preorganization, the larger the population of reactive near attack conformers.

The extent of preorganization was found to be dependent upon the enthalpy for NAC formation ($\Delta H°$) rather than phase space entropy ($T\Delta S°$). Upon comparison of the reaction activation parameters for the analogous bimolecular esterification of a carboxylic acid by an alcohol to those for the intramolecular lactonization, the advantage of the intramolecular reaction was found to reside in $\Delta H^{\ddagger}$ rather than in $T\Delta S^{\ddagger}$ (*15*). Thus, the kinetic advantage of proper preorganization in the construction of the intramolecular reactant is

[1] Abbreviations: E·S and E·TS, enzyme−substrate and enzyme−transition state complexes, respectively; NAC, near attack conformers (conformers of substrate and active site functional groups which closely resemble the transition state, reactive conformers); *P*, mole fraction of ground state conformers that are present as NACs; MD, molecular dynamics; DHFR, dihydrofolate reductase; H_2F and H_4F, dihydrofolate and tetrahydrofolate, respectively; NAD^+ and NADH, oxidized and reduced nicotinamide adenine dinucleotide; S_N2, second-order nucleophilic displacement on carbon; $S_N2(P)$, second-order nucleophilic displacement on phosphorus; AdoMet, *S*-adenosylmethionine; M.*Hhal*, cytosine methyl transferase from *Haemophilus haemolyticus*.

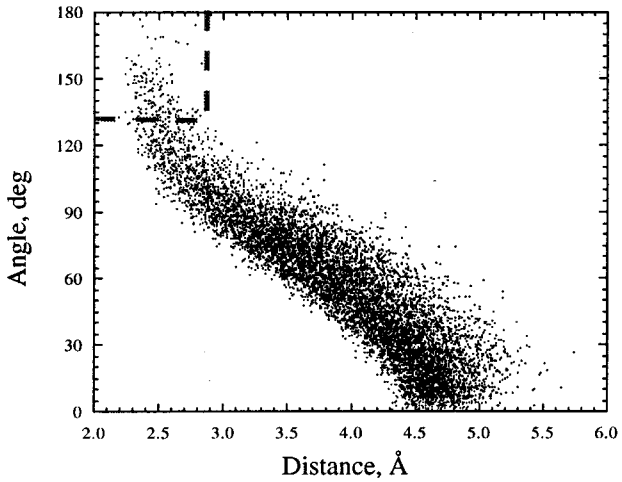

FIGURE 3: Plot of the virtual angles of approach between formate and nicotinamide [(NAD$^+$)C4−(formate)H1−(formate)C1] vs the distance between the formate hydrogen (H1) and C4 of NAD$^+$ for each of ∼9500 conformers sampled in the MD simulation of the ground state E·S of formate dehydrogenase. The conformers characterized by distances between reacting centers of ≤3.2 Å and virtual angles of 130−180° (box at the top left corner) represent NACs.

a function of enthalpy.

Use of Molecular Dynamics To Provide Descriptions of Enzyme Substrate (E·S) and Enzyme Transition State (E·TS) Structures. Sampling of the conformational space of an enzyme−substrate complex (E·S) can be accomplished by molecular dynamic (MD) simulations. To do so requires coordinates of ≤2 Å resolution. For very efficient enzymes the structural preorganization might be such that the mole fraction (*P*) of near attack conformers (NACs) in E·S approaches unity. This might be brought about by a sudden change of active site geometry upon binding S (*16*). The occurrence of only small populations of NACs among the ground state conformations of a given E·S may be due to the presence of many E·S conformations which do not differ greatly in energy. The finding of a small mole fraction of NACs does not mean that these structures are necessarily at a higher energy content than the average E·S conformation.

There have been a small number of MD calculations of NAC populations in enzyme reactions. On a nanosecond time scale the mole fraction of NACs formed in the E·S complex of catechol *O*-methyltransferase is estimated at 7.6% (*17*) while for the DNA−cytosine methylase M.*Hhal* the value of *P* is ∼1% (*18*). Similarly, a low mole fraction of NACs (1.5%) is found in the formate dehydrogenase−formate−NAD$^+$ complex (Figure 3) (*19*).

For the thermodynamically more difficult redox reactions catalyzed by nicotinamide-dependent enzymes, the mole fraction of NAC conformations is believed to be much higher. For dihydrofolate reductase ca. 20% of the NADPH·H_2F·DHFR complex is in a productive conformation over a 10 ns period. The immediate product complex (NADPH·H_4F·DHFR), however, is <10% in a reactive conformation over the same time period (*20*). In the reduction of pyruvate by NAD(P)H at the active site of dogfish lactate dehydrogenase NACs represent a mole fraction of >50% (*21*).

"Bulky amino acid side chain(s)" located on the face of the NAD(P)H distal to the substrate is (are) observed in a number of NAD(P)H enzymes (lactate dehydrogenase, Ile249 and Val36; dihydrofolate reductase, Phe102; malate dehydrogenase, Ala245 and Leu157; glyceraldehyde-3-P dehydrogenase, Ile12 and Tyr317; horse liver alcohol dehydrogenase, Val203) (*21*). The normal wagging motion of 1,4-dihydropyridines (Chart 2) is directed away from the bulky amino acid side chain(s) such that the anisotropic motion is toward the substrate and the hydrogen to be transferred (H_S or H_R) is in a quasi-axial position allowing closer approach of reactants (Chart 3, Figure 4). Both semiempirical and ab initio calculations suggest that this quasi-boat arrangement (Chart 3) results in a decrease of activation energy for hydride transfer by 4−5 kcal/mol when compared to planar NADH (*20*). With horse liver alcohol dehydrogenase, reduction in the size of the bulky amino acid side chain (Val203) results in a decrease in the rate of hydride transfer (*23*). The log(k_{cat}/K_m) decreases in a linear fashion with an increase in the MD-derived closest contact distance between reactants in single 203-position mutant structures (Figure 5) (*22*). The bulky substituents, thus, promote NAC formation. This dependence of rate on distance is anticipated and may contribute to the hydrogen tunneling observed for this class of enzymes (*22*−*24*).

The structure of NACs may differ considerably from the average conformations of E·S in an X-ray crystallographic structure due to crystal packing forces or interactions between enzyme structures in the crystal. A case in point is the self-cleavage of the RNA hammerhead ribozyme (*25*). In an unconstrained nanosecond MD simulation in water, the hammerhead, with Mg^{2+} ligated to the *pro-R* oxygen of the

Chart 2

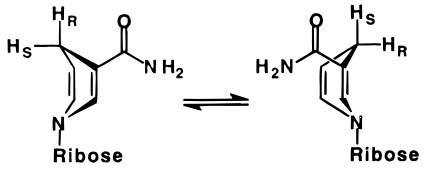

Chart 3

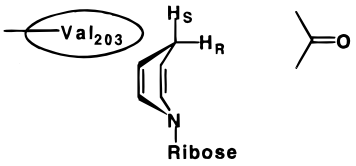

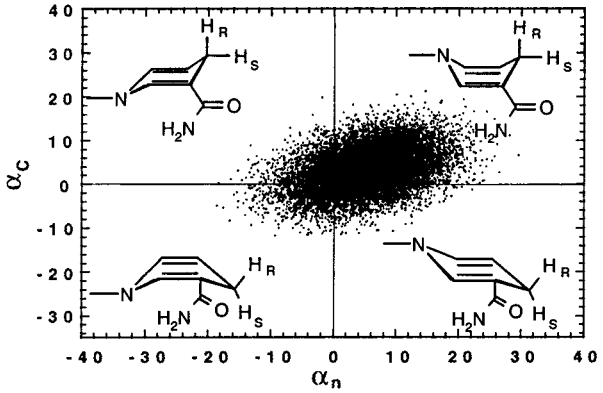

FIGURE 4: Anisotropic bending conformers of the NADH in the HLADH·NADH·PhCHO complex from MD simulations. The angles α_C and α_N represent the bending out of plane for C4 and N1, respectively.

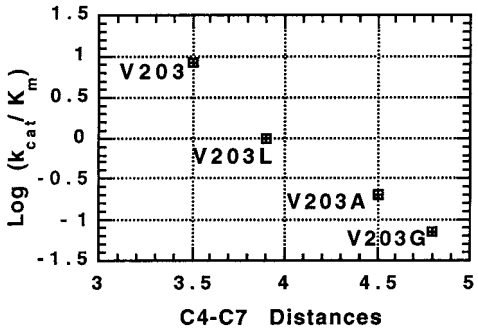

FIGURE 5: Catalytic efficiency (k_{cat}/K_m) of HLADH as a function of close contact distance between C4 of NAD^+ and C7 of $PhCH_2$-OH for wild-type Val203 and single point mutants. Values of k_{cat}/K_m are from the literature (*19*, *21*), and the distances are from MD simulations.

phosphodiester bond to be cleaved, undergoes conformational changes which allow formation of NACs. These NACs, which are present up to 18% of the time (*26*), allow the inline $S_N2(P)$ attack of (C17)ribose-2′O^- on the 3′-phosphodiester phosphorus with displacement of (A1.1)ribose-5′O^-. NAC formation follows the turning out of the C17 nucleobase and a flip of the ribose conformation from C3′-*endo* to C2′-*endo*. These changes are possible, in part, because interactions within the crystal structure are removed.

Up to this point, we have considered the ground state conformations which are formed after bringing together of reactants in intramolecular and enzymatic reactions and the influence of active site's preorganization on the formation of reactive conformations (NACs). Further considerations relate to the characteristics of enzymes that assist the conversion of a E·NAC to E·TS. Because chemical reactions within E·S complexes generally occur on a millisecond time scale, there is sufficient time for many conformational changes to occur that could induce the reaction. However, because the NAC conformations are so similar to the structure of the TS, it is not expected that the protein will undergo significant changes in structure on conversion of E·NAC to E·TS (*19*). Only minor changes in side chain orientation and in the position of water molecules are contemplated (*19*). The organization of the enzyme structure places the amino acid side chains, which will be involved in the formation of the TS (general bases, general acids, nucleophiles, and the solvent milieu), in correct position on formation of the E·NAC complex (*6*, *27*). The reorganization energy of orienting polar groups in the conversion of E·NAC to E·TS is small, relative to the reaction in solution (*28*, *29*) because the dipoles are already fixed in the NAC to interact with the TS. To this, we would add that changes in electron densities on conversion of NAC to TS will be correlated with changes in the lengths of electrostatic interactions with enzyme functional groups. From this perspective, extending the lifetime of the transition state, which in a chemical reaction is about 10^{-13} s (*30*, *31*), through protein domain motions is unlikely because the only changes in structure of the protein, aside from water migration, on E·NAC conversion to E·TS, are the lengthening and shortening of electrostatic and dipolar interactions.

Just as the conformations of substrate and enzyme in the E·S complex can be simulated by MD calculations so may the E·TS complex, providing that the geometry and charge distribution of the enzyme-bound TS is known. Isotope effects determined at many atoms of the substrate allow calculation of the TS structure. For a particular type of mechanism, such as some S_N2 reactions (*32*), the relative kinetic isotope effects are insensitive to the solvent environment, and hence, the structure of TS is not dependent on the surrounding dielectric. In such a situation, it would be fair to assume that the TS in E·TS could be approximated by the ab initio gas-phase TS. Ab initio calculated TS structures should resemble the TS of the enzyme reaction when the experimental and calculated heavy atom ($^{13}C/^{12}C$ and $^{15}N/^{14}N$) isotope effects are the same. The calculated and experimental values of $^{13}C/^{12}C$, as well as $^3H/^1H$, are the same for the catechol *O*-methyltransferase reaction (*33*). Alternatively, one may calculate enzyme-bound transition state structures using programs in which the force field of the enzyme is expressed by molecular mechanics (MM) and the reaction trajectory and TS structure are computed by quantum mechanics (QM) (*34*). Calculations with standard ab initio and semiempirical QM methods do not provide contributions of tunneling (H^- and H^+) to the activation energy (*35*); however, the contribution does not greatly affect $\Delta G^‡$ (*36*, *37*).

Table 2: Solvent Dependence of the S_N2 Reaction[a]
$Cl^- + CH_3Br \rightarrow ClCH_3 + Br^-$

solvent	dielectric ϵ	relative rates (cm^3 $molecule^{-1}$ s^{-1})
gas phase	1	1.0
Me_2CO	20.7	10^{-10}
DMF	38.3	10^{-11}
CH_3OH	32.6	10^{-15}
H_2O	78.4	10^{-16}

[a] See ref 40.

The rates of many polar reactions, however, are markedly influenced by the dielectric and structure of the solvent in which the reactions are carried out. There may be large changes in solvation of a substrate upon transfer from water to the interior of an enzyme (*29*). Consequently, a significant amount of catalysis may be accounted for by a preorganized active site environment complementary to the TS that avoids the large solvent reorganization energies of the solution reaction (*5*, *26*, *38*). Removal of the solvent reorganization energy lowers the activation energy and is conceptually different than lowering the activation energy by binding the TS. When conducive to lowering the barrier for reaction, the active site of a given enzyme may be almost hydrocarbon in nature. Alternatively, arrangement of polar side chains and peptide bonds may be such that the active site is a heterogeneous polar matrix providing prearranged electrostatic interactions with the substrate and transition state. For S_N2 displacement reactions, involving negatively charged nucleophile and leaving group, the calculated gas-phase transition state structures do not differ from those determined in solution (*32*, *39*), although the rate constants are 10^{11}–10^{17}-fold greater in the gas phase (*40*) (Table 2). The decrease in rate in solution is related to an increase in the polarity of the solvent (ϵ) as well as the ability of the solvent to form hydrogen bonds with reactants (i.e., hindrance of reaction by solvation of reacting centers).

We will now review the results of computation analysis applied to several enzymes. The *Xanthobacter autotrophicus* haloalkane dehalogenase reaction features nucleophilic attack

by Asp124−CO_2^- upon 1,2-dichloroethane to provide Asp124−CO_2−CH_2CH_2−Cl + Cl^- (*41*−*43*). The substrate is surrounded by 14 nonpolar amino acid side chains. The catalytic influence of this enzyme revolves around the creation of NAC structures in the Michaelis complex. In the preorganized active site the carboxylate nucleophile of Asp124 is held in place in the NAC structure by hydrogen bonds involving two backbone amide hydrogens of Glu56 and Trp125 and a water molecule. The 1,2-dichloroethane is maintained in the gauche conformation needed to form the TS, and the Cl− substituent to be displaced is hydrogen bonded to the indole NH of Trp125. On formation of the transition state the hydrogen bond between water and the caboxylate nucleophile is lost while a new hydrogen bond between the incipient leaving Cl^- by Trp175 is formed. The lyophobic surrounding of the active site lowers the internal dielectric and ensures the hydrogen bonds from the four HN< functions to be sufficiently strong. The additional hydrogen bond, involving Trp175, present in the TS has only a moderate influence on rate (*44*). Transition state binding, as compared to NAC binding, cannot be responsible for the full catalytic advantage of this enzyme. The single electrostatic interaction present in the TS that is not present in the ground state (Trp175) is balanced by an interaction in the ground state (H_2O) that is not present in the TS.

Identical reasoning can be applied to the reactions catalyzed by staphylococcal nuclease and orotidine-5-monophosphate decarboxylase that have the largest rate accelerations measured to date. In both cases, calculations have shown that the model solution reaction rates can be increased by $>10^{17}$ by desolvation of substrate and preorganizing the active site by strategically placing weak acids and/or bases in the low dielectric environment (*45*).

MD simulations of both ground and transition states are possible with formate dehydrogenase since the structure of the TS is known from the identity of calculated and experimental isotope effects (loc. cit.). In the E·NAC, there are a total of 11 electrostatic interactions with the formate and nicotinamide of NAD^+ (*18*). The 11 electrostatic interactions persist in E·TS. The nature of the 11 electrostatic interactions on going from E·NAC to E·TS differs in that the bifurcated hydrogen bonds between the positively charged guanidino group of Arg284 and the negative formate oxygen lengthen by ∼0.4 Å and the hydrogen bond between the nicotinamide amide carbonyl oxygen and the imidazole of His332 decreases by ∼0.5 Å. These changes are expected since the negative charge on the formate carboxyl oxygen is diminished (eq 1) upon conversion of E·S to E·TS and

$$NAD^+ + H{-}CO_2^- \rightarrow NADH + CO_2 \qquad (1)$$

the electron density of the nicotinamide amide carbonyl is increased (Scheme 2). This observation supports the statement "substrate ground state−enzyme interactions and transition state−enzyme interactions in general often differ by only the increased dipolar nature of the bond undergoing transition within the active site" (*6*). The simulations show that the transition state in formate dehydrogenase is not held by the enzyme more tightly than the ground state NAC, and the enzyme can distinguish between NAC and TS structures.

The carbamoyl synthetase small subunit catalyzes the hydrolysis of glutamine [$NH_2C(O)$−R] by a two-step mechanism, involving attack of Cys269−S^- to provide a tetrahedral intermediate which gives way to the thioester Cys269−S−C(O)−R followed by hydrolysis of the latter. Crystal structures of the E·S complex of an analogue model of the tetrahedral intermediate and of the thiolester product of the first step of reaction allow the comparison of 10 electrostatic interactions during the reaction (*45*). The separation within their electrostatic interactions differs little in going from reactants to intermediate to ptoduct. On this basis it has been concluded that this reaction is not driven by transition state binding.

Scheme 2

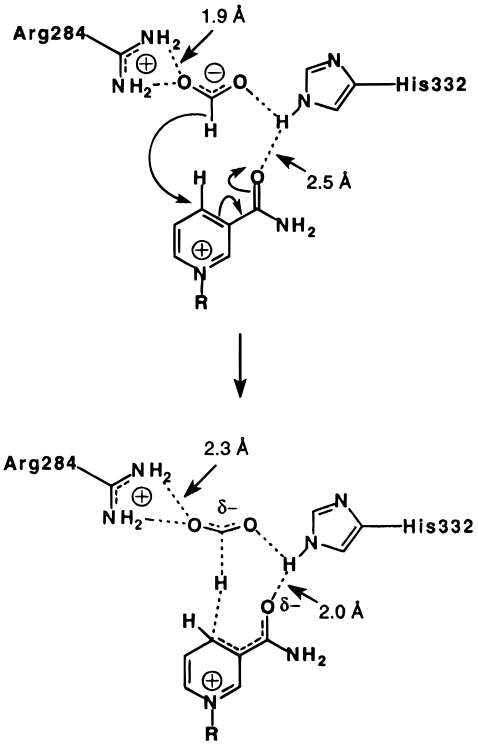

The source of the enormous rate acceleration (estimated at 10^{16}) (*46*) by the enzyme catechol *O*-methyltransferase appears to be related to the enzyme's ability to desolvate the substrate and orient the two reactants into a NAC. This conclusion is strongly supported by both molecular dynamic simulations and ab initio computations. The placement of enzyme side chains in the E·TS and E·NAC is essentially the same. In the absence of enzyme, the ab initio gas-phase reaction faces an activation barrier of 22−23 kcal/mol, and similar activation barriers have been observed in solution for the methylation of phenol by models of AdoMet (*47*). However, a dramatic reduction of the activation barrier to 3−5 kcal/mol was found when the ab initio optimized ground state structure was replaced by a NAC (*48*).

MD simulations of E·S and E·TS indicate that the three active site residues, Met40, Tyr68, and Asp141, assist in positioning the AdoMet so that the methyl group is in the vicinity of the catecholate oxygen to provide a NAC. Interestingly, MP2/6-31+G(d,p) calculations showed that all three residues interact more strongly with the ground state than with the transition state (*48*). The placement of the catecholate oxygen nucleophile and AdoMet methyl group and their distance apart are affected by a correlated clamping motion of the catecholate and Tyr68 so as to form a NAC

by pushing the reactants together (*17*). These studies support a lack of preferential transition state binding in the catechol *O*-methyltransferase reaction.

Enzymatic Binding of Transition State Analogues and Transition States. Evidence presented so far contradicts the general precept that the catalytic efficiency of enzymes *requires* the tighter binding of transition states compared to ground states. For the few enzymes examined, the reactive ground state conformers (NACs) and transition states exhibit comparable overall electrostatic interactions at the active site. Studies with so-called "transition state inhibitors, mimics, or analogues" have been offered in support of the transition state binding precept. The observation that experimental values of log K_i for transition state inhibitors show an apparent correlation with log k_{cat}/K_m has been invoked as supporting the Pauling hypothesis, but we note that the correlation does not extend to k_{cat} (*49*).

Transition state mimics, by definition, must incorporate all of the substrate elements within a single molecule for bimolecular and higher order reactions and, thus, enjoy a more favorable binding to an enzyme than the individual components. The equilibrium constants for binding of transition state analogue inhibitors, in such reactions, may not reflect interactions of the enzyme's active site with the transition state. Even with enzymes whose rate-limiting step approaches substrate diffusion, there are examples of transition state inhibitors whose binding is multistep, involving slow conformational changes and very slow on and off rates. Perhaps an analogy is slipping one's foot into or out of a shoe when the laces are tied—the on and off rates are slow.

As we noted earlier, determination of the intrinsic kinetic isotope effects at multiple sites on the substrate permits a description of the transition state structure for the enzymatic reaction and the calculation of the molecular electrostatic potential at the transition state surface (*3*, *8*). Evidence that the active sites of enzymes are electrostatically and sterically complementary to transition state structures has been obtained from the comparison of the molecular electrostatic potential surfaces of transition states and transition state analogues. For the two enzymes that use the common nucleotide substrate, adenosine monophosphate, nucleotide hydrolase, and purine nucleoside phosphorylase the electrostatic potential surface of the TS more closely matches that of transition state analogues rather than substrates (*12*). That the surfaces of the active site and transition state are complementary is to be expected just as is the complementary relationship between NAC and the active site with both NACs and transition states being accommodated by simply adjusting the distances for electrostatic and dipolar interactions.

A large class of enzymes are responsible for cleavage of bonds to the C1 of cyclic hexose and ribose moieties. These reactions involve neutral substrate and products but positively charged oxocarbenium ion transition states. Oxocarbenium ions cannot form in a low dielectric without a neighboring negative counterion, so that positioned in these active sites are one or two carboxylate anions. Positively charged TS inhibitors bind tightly at the active site because of the shape and their electrostatic attraction to the carboxylate counteranions (*12*). To ascribe the electrostatic catalysis of the formation of oxocarbenium ion TS as catalysis by enzyme tight binding of the TS is imprecise and rather misleading. Compare to the enzyme-catalyzed methyl transfer reactions of AdoMet in which a highly charged ground state gives way to a TS in which there is annihilation of charge and a backing off of enzyme substituents (*38*, *50*). A better understanding of the importance of TS inhibitors to the problem should be made by comparing MD simulations of the E·S, E·TS inhibitor, and E·TS complexes for enzymes such as purine nucleosidase (*51*) and hypoxanthine−guanine−xanthine phosphoribosyltransferase (*52*).

Protein Dynamic Motions and Efficiency of Enzyme Catalysis. Almost 60 years ago Kramers suggested (with some freedom of language) that dynamic fluctuations are used by enzymes to organize the initial enzyme−substrate complex into a reactive conformation and that fluctuations away from the average ground state configuration lead to passage through the transition state (*53*). From the MD investigations reported here, we know that the Brownian motions at the active site give rise to NACs. These random thermal motions will eventually cause the transformation of NAC to TS, as in nonenzymatic reactions (*54*). Of great interest at present is the influence of motions directed at great distances from the active site in the formation of the transition state. Following the formation of NACs, in which reacting centers are at ∼3 Å separation, by the enzymes stochastic thermal motions, one can easily imagine that a sudden correlative motion initiated at a distance from the active site moves the reacting centers toward each other by 0.2−0.3 Å.

NMR studies have been used to examine (*55*) correlated motions on a time scale ranging from ∼30 ps to 6 ns. Slow, large-scale conformational fluctuations occur on the microsecond to millisecond time scale (see ref *56* and literature provided therein). These slow conformational fluctuations pertain to domain motions and should have little to do with catalysis involving efficient enzymes. Transmission of motions to remote portions of an enzyme has been observed (*57*, *58*) by MD simulations that also duplicate correlated intramolecular motions measured by NMR and X-ray (*59*, *60*). From the nature of the motions it has been inferred that they are important for catalysis (*61*−*63*).

It has been estimated that MD simulation of a protein of moderate size should be extended to about 100 ns to sample all conformations (*64*). MD simulations of E·S complexes in explicit solvent have been carried out to 10 ns (*20*) while the majority of studies only extend to 1 or 2 ns. There is, at present however, little direct evidence as to how enzymes use correlated motions in catalysis. Theoretical treatments have been offered which explicitly recognize the role of protein dynamics in the treatment of hydride transfer reactions and tunneling (*56*, *62*).

Correlated motions are believed to decay over a correlation length of 4−8 Å (*65*). However, the dynamic motions of the βF,βG loop observed for the dihydrofolate reductase−folate complex (*59*), by ^{15}N NMR, are linked to the active site over a distance of ∼13 Å. In the dihydrofolate reductase reaction, this correlative motion is profoundly associated with the various steps of the catalytic reaction that transforms substrate to product. A single point mutation Gly120Val disrupts the normal frequency motions of the βF,βG loop and, likewise, interferes with the conversion of the initial ternary enzyme−substrate−cofactor complex to the Michaelis complex, so that this step becomes partially rate limiting

relative to the wild-type enzyme, reducing the hydride transfer step by ca. 500-fold. Molecular dynamics calculations, however, reveal that the fraction of substrate molecules existing as NACs within the ternary complex is the same for both the mutant and the wild-type enzyme (*66*). One interpretation of the collective data is that correlated motions in this region of the protein are acting to increase the frequency of barrier crossing and may contribute several orders of magnitude to increasing enzyme turnover efficiency.

Conclusions. The two concepts most applied when discussing the efficiency of enzymes as catalysts are (i) enzymes lower the free energy barrier in catalysis by having a considerably greater affinity for transition state (E·TS) compared to ground state (E·S) and/or (ii) enzyme catalysis is principally driven by the gain in entropy over the comparable nonenzymatic reaction. Recently generated evidence calls into question the universality of these two precepts. The value of the constant K_{TS} should not be viewed as a true measure of the dissociation constant for E·TS (Scheme 1) but as an estimate for the efficiency of enzyme catalysis due to all those entities involved in both the nonenzymatic and the enzymatic reaction (solvation, etc.). The increase in rate constants in comparing a number of first-order spontaneous reactions in water to their enzyme-catalyzed counterpart has been found, experimentally, to arise in the change of enthalpy of activation ($\Delta\Delta H^{\ddagger}$) rather than the entropy of activation ($\Delta T\Delta S^{\ddagger}$).

The preorganization of the enzyme active site to promote the formation of NACs is a critical component of enzyme catalysis. In an example of intramolecular reactions involving a common transition state, the efficiency of this preorganization is reflected in the ground state enthalpy ($\Delta H°$), and the differences in the rates of reaction due to preorganization are determined by $\Delta H^{\ddagger}$. At best, one must prove experimentally that an increase in $T\Delta S^{\ddagger}$ is mainly responsible for the efficiency of a given enzyme.

In the computational examination of enzyme catalysis, the favored procedure is to use molecular dynamics (MD) to examine all conformations of E·S. Those conformers for which the reacting atoms are at a distance of combined van der Waals radii (at ambient temperatures) or ~0.4 Å less and angles within ±15° of the bonding angle in the transition state are the reactive ground states (NACs). The population of NACs within E·S can be easily calculated. The MD-based generation of a large family of E·S structures including NACs is preferable over a quantum mechanical optimization of a bimolecular complex as the latter neglects protein environment and produces only a single structure. When the structure of the transition state can be deduced from kinetic isotope effects, MD simulations of E·TS will provide those conformations of the enzyme that will support the transition state. From a comparison of E·NAC and E·TS structures one can determine differences in ground state and transition state binding by enzyme. Further, by use of QM/MM calculations and umbrella sampling one may calculate the free energy difference between NAC and TS. Finding that E·S exists only a small portion of the time as a NAC does not mean that NAC structures are at a higher energy level than the average E·S structure because of the many conformations of E·S with like stability. This feature is difficult to portray in a two-dimensional reaction coordinate diagram. For a given enzyme, the difference in structure of NAC conformations is small, but these small differences may be reflected, to some extent, in the generation of transition states which also differ slightly in structure (*51*).

For the few enzymes for which ground state and transition state enzyme conformations have been examined by MD simulations [catecholate *O*-methyltransferase (*33*), formate dehydrogenase (*19*), and *Xanthobacter autotrophicus* haloalkane dehalogenase (*42*)], it is found that transition state binding by enzyme is comparable to ground state binding of NACs. Thus, in these cases marked preferential binding of TS over ground state NACs is not requisite for catalytic activity. It remains to be seen how various enzymes will divide into classes distinguished by the relative contributions of ground versus transition state to catalysis, and this remains a fertile field for exploration.

The establishment of correlative motions in enzymes has led to speculations as to their role in catalysis. Correlative motions appear to participate in the formation of NACs in the catechol *O*-methyltransferase E·S complex and in the rate of turnover of dihydrofolate reduction. The blocking of such motion, as in the case of the dihydrofolate reductase−folate complex, by a single mutation imposes profound changes on all steps of the reaction and has stimulated the belief that correlative motions can provide a thermal activation activity (*66*).

Epilogue. It is appropriate to provide a retrospective of the thoughts concerning "the driving forces" in enzyme catalysis as they have evolved during the last 50 years. The term propinquity (proximity) was applied by Lumry (1959) to the driving force in enzyme catalysis brought about by bringing the substrate and active site together, thereby increasing (i) the collision frequency of reactants (entropy) or (ii) the holding together of reactant in a restricted geometry (enthalpy) (*67*). The enthalpy-driven NAC formation now appears to be of major importance. The terms "proximity effect" and "propinquity effect" were also applied by us to studies of intramolecular reactions designed to model enzyme catalysis (ref *68* and citations therein; ref *69*, Chapter 1). When originally reported, the order of the rate constants of the intramolecular reactions of Figure 2 was rationalized in terms of manipulating ground states to force the reactant terminals together. The rate enhancement of 10^8, over the numerical value of the rate constant for the bimolecular reaction (Figure 2), was proposed to arise from a transition from an extended to a closed conformation within the series of dicarboxylic acid nonesters, with the latter being close in structure to the transition state. As others have observed, there is no general need to postulate "different chemistry" (*70*). It was concluded (in 1960) (*71*) that the numerical rate enhancement of 10^8 "point to the tremendous enhancement of rate that an enzyme could achieve by *fixing* the reacting species in a *steric conformation closely resembling* that of the *transition state* for the reaction". Menger was to reiterate this proposal of holding the substrate in a reactive conformation some quarter century latter (*72*−*74*). It is gratifying that modern computational results support the intuitive conclusions of 40 years past.

REFERENCES

1. Pauling, L. (1946) *Chem. Eng. News 24*, 1375.
2. Pauling, L. (1948) *Nature 161*, 707−709.

3. Radzicka, A., and Wolfenden, R. (1995) *Science 265*, 90−93.
4. Schowen, R. L. (1978) *Transition State of Biochemical Processses*, Chapter 2, Plenum Press, New York.
5. Cannon, W. R., and Benkovic, S. J. (1998) *J. Biol. Chem. 273*, 26257−26250.
6. Cannon, W. R., Singelton, S. F., and Benkovic, S. J. (1996) *Nat. Struct. Biol. 3*, 821−833.
7. Bruice, T. C., and Lightstone, F. C. (1999) *Acc. Chem. Res. 32*, 127−136.
8. Wolfenden, R., Snider, M., Ridgway, C., and Miller, B. (1999) *J. Am. Chem. Soc. 121*, 7419−7420.
9. Hammes, G. G. (1963) *Nature 204*, 342−343.
10. Jencks, W. P. (1975) *Adv. Enzymol. 43*, 219−310.
11. Koshland, D. E. (1958) *Proc. Natl. Acad. Sci. U.S.A. 44*, 98−104.
12. Schramm, V. L. (1998) *Annu. Rev. Biochem. 67*, 693−720.
13. Lightstone, F. C., and Bruice, T. C. (1996) *J. Am. Chem. Soc. 118*, 2595−2605.
14. Lightstone, F. C., and Bruice, T. C. (1997) *J. Am. Chem. Soc. 119*, 9103−9113.
15. Lightstone, F. C., and Bruice, T. C. (1998) *Bioorg. Chem. 26*, 193−199.
16. Westheimer, F. (1962) *Adv. Enzymol. 24*, 441−482.
17. Lau, E., and Bruice, T. C. (1998) *J. Am. Chem. Soc. 120*, 12387−12394.
18. Lau, E., and Bruice, T. C. (1999) *J. Mol. Biol. 293*, 9−18.
19. Torres, R., Schøtt, B., and Bruice, T. C. (1999) *J. Am. Chem. Soc. 121*, 8164−8173.
20. Radkiewicz, J. L., and Brooks, C. L. (2000) *J. Am. Chem. Soc. 122*, 225−231.
21. Almarsson, O., and Bruice, T. C. (1993) *J. Am. Chem. Soc. 115*, 2125−2138.
22. Bahnson, B. L., Park, D.-H., Kim, K., Plapp, B. V., and Klinman, J. P. (1993) *Biochemistry 32*, 5503−5507.
23. Luo, J., Kahn, K., and Bruice, T. C. (1999) *Bioorg. Chem. 27*, 289−296.
24. Bahnson, B. J., Colby, T. D., Chin, J. K., Goldstein, B. M., and Klinman, J. P. (1997) *Proc. Natl. Acad. Sci. U.S.A. 94*, 12797−12802.
25. Scott, W. G., Murray, J. B., Arnold, J. R. P., Stoddard, B. L., Klug, A. (1996) *Science 274*, 2065−2069.
26. Torres, R. A., and Bruice, T. C. (2000) *J. Am. Chem. Soc. 122*, 781−791.
27. Warshel, A. (1998) *J. Biol. Chem. 273*, 27035−27038.
28. Warshel, A., and Florian, J. (1998) *Proc. Natl. Acad. Sci. U.S.A. 95*, 5950−5955.
29. Warshel, A. (1978) *Proc. Natl. Acad. Sci. U.S.A. 75*, 5250−5254.
30. Truhlar, D. G., Hase, W. L., and Hynes, J. T. (1983) *J. Phys. Chem. 87*, 2664−2682.
31. Albery, W. J. (1993) *Adv. Phys. Org. Chem. 28*, 138−170.
32. Shaik, S. S., Schlegel, H. B., and Wolfe, S. (1992) *Theoretical Aspects of Physical Organic Chemistry. The S_N2 Mechanism*, Chapter 5, John Wiley & Sons, New York.
33. Zheng, Y.-J., and Bruice, T. C. (1997) *J. Am. Chem. Soc. 119*, 8137−8145.
34. Monard, G., and Merz, K. M. (1999) *Acc. Chem. Res. 32*, 904−911.
35. Alhambra, C., Gao, J., Corchado, J. C., Villa, J., and Truhlar, D. G. (1999) *J. Am. Chem. Soc. 121*, 2253−2258.
36. Northop, D. B. (1999) *J. Am. Chem. Soc. 121*, 3521−3524.
37. Northop, D. B., and Cho, Y.-K. (2000) *Biochemistry 39*, 2406−2412.
38. Kuhn, B., and Kollman, P. A. (2000) *J. Am. Chem. Soc. 122*, 2586−2596.
39. Westaway, K. C. (1987) in *Isotopes in Organic Chemistry* (Buncel, E., and Lee, C. C., Eds.) Vol. 7, Elsevier, New York.
40. Tanaka, K., Mackay, G. I., Payzant, J. P., and Bohme, D. K. (1976) *Can. J. Chem. 54*, 1643−1659.
41. Verschueren, K. H. G., Kingma, J., Rozeboom, H. J., Kalk, K. H., Janssen, D. B., and Dijkstra, B. W. (1993) *Biochemistry 32*, 9031−9037.
42. Lightstone, F. C., Zheng, Y.-J., and Bruice, T. C. (1998) *Bioorg. Chem. 26*, 169−174.
43. Lightstone, F. C., Zheng, Y.-J., Bruice, T. C. (1998) *J. Am. Chem. Soc. 120*, 5611−5621.
44. Schindler, J. F., Naranjo, P. A., Honaberger, D. A., Chang, C.-H., Brainard, J. R., Vanderberg, L. A., and Unkefer, C. J. (1999) *Biochemistry 38*, 5772−5778.
45. Thoden, J. B., Huang, X., Raushel, F. M., and Holden, H. M. (1999) *Biochemistry 38*, 16158−16166.
46. Mihel, I., Knipe, J. O., Coward, J. K., and Schowen, R. L. (1979) *J. Am. Chem. Soc. 101*, 4349−4351.
47. Swain, C. G., and Taylor, L. J. (1962) *J. Am. Chem. Soc. 84*, 2456−2457.
48. Kahn, K., and Bruice, T. C. (2000) *J. Am. Chem. Soc. 122*, 46−51.
49. Phillips, M. A., Kaplan, A. P., Rutter, W. J., and Bartlett, P. A. (1992) *Biochemistry 31*, 959−963.
50. Lau, E., and Bruice, T. C. (2000) *J. Am. Chem. Soc.* (submitted for publication).
51. Degano, M., Almo, S. C., Sacchettini, J. C., and Schramm, V. L. (1998) *Biochemistry 37*, 6277−6285.
52. Shi, W., Li, C. M., Tyler, P. C., Furneaux, R. H., Cahill, S. M., Girnin, M. E., Grubmeyer, C., Schramm, V. L., and Almo, S. C. (1999) *Biochemistry 38*, 9872−9880.
53. Kramers, H. A. (1940) *Physics 7*, 284.
54. Hammes, G. G. (1968) *Acc. Chem. Res. 1*, 321−329.
55. van Aalten, D. M. F., Hoff, W. D., Findlay, J. B. C., Crielaard, W. C., and Hollongwerf, K. J. (1998) *Protein Eng. 11*, 875−879.
56. Bruno, W. J., and Bialete, W. (1992) *Biophys. J. 63*, 689−699.
57. Lau, E. Y., and Bruice, T. C. (1999) *Biophys. J. 77*, 85−98.
58. Epstein, D. M., Benkovic, S. J., and Wright, P. E. (1995) *Biochemistry 34*, 11037−11048.
59. Faure, P., Micur, A., Perahia, D., Doucet, J., Smith, J. C., and Benoit, M. (1994) *Struct. Biol. 1*, 124−128.
60. Horstink, L. M., Abseher, R., Nilges, M., and Hilbers, C. W. (1999) *J. Mol. Biol. 287*, 569−577.
61. Holland, D. R., Tronrud, D. E., Pley, H. W., Flaherty, K. M., Stark, W., Jansonius, J. N., McKay, D. B., and Mathews, B. W. (1992) *Biochemistry 31*, 11310−11316.
62. Farnum, M. F., Magde, D., Howell, L. E., Hirai, J. T., Warren, M. S., Grimsley, J. K., and Kraut, J. (1991) *Biochemistry 30*, 11567−11579.
63. Bahar, I., Erman, B., Jernigan, R. L., Atilgam, A. R., and Covell, D. G. (1999) *J. Mol. Biol. 285*, 1023−1037.
64. Clarage, J. B., Romo, T., Andrews, B. K., Pettitt, B. M., and Phillips, G. N. (1995) *Proc. Natl. Acad. Sci. U.S.A. 92*, 3288−3292.
65. (a) Antoniou, D., and Schwartz, S. D. (1997) *Proc. Natl. Acad. Sci. U.S.A. 94*, 12360−12365; (b) Castillo, R., Andrés, J., and Moliner, V. (1999) *J. Am. Chem. Soc. 121*, 12140−12147.
66. Miller, G. P., and Benkovic, S. J. (1998) *Chem. Biol. 5*, R105−R113.
67. Lumry, R. (1959) in *The Enzymes* (Boyer, P. D., Lardy, H., and Myrback, K., Eds.) 2nd ed., Vol. 1, pp 157−228, Academic Press, New York.
68. Bruice, T. C. (1976) *Annu. Rev. Biochem. 45*, 331−373.
69. Bruice, T. C., and Benkovic, S. J. (1996) *Bioorganic Mechanisms*, Vol. I and II, W. A. Benjamin Inc., New York.
70. Scrutton, H., Basran, J., and Suteliffe, M. J. (1999) *Eur. J. Biochem. 264*, 666−671.
71. Knowles, W. P. (1991) *Nature 350*, 121−124.
72. Bruice, T. C., and Pandit, U. K. (1960) *Proc. Natl. Acad. Sci. U.S.A. 46*, 402−404.
73. Menger, F. M. (1985) *Acc. Chem. Res. 18*, 128−134.
74. Menger, F. M. (1993) *Acc. Chem. Res. 26*, 206−212.
75. Khanijin, N. A., Snyder, J. P., and Menger, F. M. (1999) *J. Am. Chem. Soc. 121*, 11831−11846.

BI0003689